electronics

Article

Reconfigurable Antennas for RF Energy Harvesting Application: Current Trends, Challenges, and Solutions from Design Perspective

Bikash Ranjan Behera [1], Sanjeev Kumar Mishra [2], Mohammed H. Alsharif [3,*] and Abu Jahid [4,*]

[1] Department of Electronics & Communication Engineering, Vel Tech Rangarajan Dr. Sagunthala R&D Institute of Science and Technology (Deemed-To-Be-University), Chennai 600062, Tamil Nadu, India; drbikash@veltech.edu.in
[2] Advanced RF and Microwave Engineering Lab, Department of Electronics and Communication Engineering, International Institute of Information Technology (IIIT) Bhubaneswar, Bhubaneswar 751003, Odisha, India; sanjeev@iiit-bh.ac.in
[3] Department of Electrical Engineering, College of Electronics and Information Engineering, Sejong University, Seoul 05006, Republic of Korea
[4] School of Electrical Engineering and Computer Science, University of Ottawa, 25 Templeton St., Ottawa, ON K1N 6N5, Canada
* Correspondence: malsharif@sejong.ac.kr (M.H.A.); ajahi011@uottawa.ca (A.J.)

Abstract: Due to the widespread use of low-power embedded devices in both industrial and consumer applications, research into the use of alternate energy sources has been sparked by the requirement for continuous power. Due to its accessibility and ability to be implanted, RF energy is always taken into consideration among the traditional energy sources that are currently available. There is a significant necessity for efficient RF front-ends, which must provide effective circular polarization (CP) features, effectiveness, feasibility from a design standpoint, and optimal usage of ambient RF signals accessible in the environment. So, for understanding their utilization in RF energy harvesting, a metasurface reflector-inspired CP-printed reconfigurable antenna integrated with a Greinacher voltage divider (GVD) rectifier circuit is reported. It offers broadband CP with fractional bandwidth > 25%, CP gain > 8.35 dBic, and directional radiation with the 3 dB angular beamwidth > 100° in the 3.5/5 GHz bands. With the integration of the rectifier circuit, a theoretical DC output > 4.8 V at 12 dBm is obtained. The acceptable impedance bandwidth, axial ratio bandwidth, antenna gain, antenna efficiency, and directional radiation with a 3 dB angular beamwidth value are studied and subsequently matched with the trade-offs (usage of diodes, complexity of DC biasing circuits, and attainment of polarization reconfigurability) obtained from the state of the art. A comprehensive study of the reconfigurable antennas is reported to highlight the findings as a widespread solution for these limitations in RF energy harvesting application.

Keywords: circular polarization; directional pattern; metasurfaces; printed monopole antenna; reconfigurability; RF energy harvesting

Citation: Behera, B.R.; Mishra, S.K.; Alsharif, M.H.; Jahid, A. Reconfigurable Antennas for RF Energy Harvesting Application: Current Trends, Challenges, and Solutions from Design Perspective. *Electronics* **2023**, *12*, 2723. https://doi.org/10.3390/electronics12122723

Academic Editor: Giovanni Leone

Received: 22 May 2023
Revised: 14 June 2023
Accepted: 16 June 2023
Published: 18 June 2023

1. Introduction

The purpose of this particular review article is to provide a comparative focus on the probable utilization of reconfigurable antennas integrated with the rectifier circuit for the purposes of energy harvesting applications. In general, the user-friendliness of RF energy harvesting technology, which is accomplished through the utilization of ambient RF signals, has paved the way for a way to save costs and eliminate the requirement for periodic maintenance with regard to the device. The many different kinds of environmental energy sources that are currently accessible are disregarded as possibilities. Among them, the potential of radio frequency (RF) energy as the possible alternative source of energy for replacing batteries in sensors is determined to be superior. This is because it is typically implemented with the assistance of the internet of things (IoT) and wireless sensor networks (WSNs), for the various applications [1,2]. So, with the demand for low-power embedded devices (LPEDs), there is a need for research directed towards the improvement of power requirements for the particular scenario [3,4] when there is the involvement of multi-functional electronic components [5–10]. For this type of environment, we require a battery-less operation due to their limited lifespans. Additionally, one of the major limitations is the processing of battery waste, which ends up in a landfill. It becomes worse because a large number of embedded devices are used in our day-to-day life for different activities, where the battery is the only energy source for their operation. So, the phenomenon of RF energy harvesting (i.e., shown in Figure 1 and Table 1) has become an appealing prospect for reducing cost and the requirement for periodic maintenance at regular intervals, making the devices self-sustaining in nature.

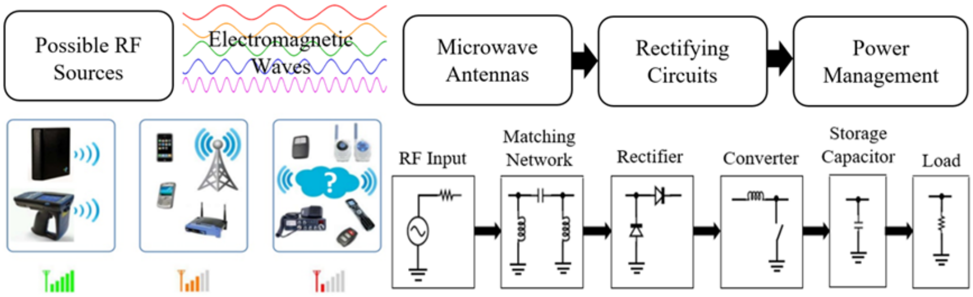

Figure 1. Constituent elements of RF energy harvesting (RF-EH) system [7].

Table 1. List of commercially available RF energy sources [7] (information about emission power levels is decided by the Federal Communication Committee).

Sources	Frequency of Operation	Emission Power Levels	Utilization
FM Tower	88–108 MHz	−36 dBm to +36 dBm	WPTs
TV Tower	180–220 MHz	−36 dBm to +36 dBm	WPTs
AM Tower	530–1620 MHz	−36 dBm to +36 dBm	WPTs
CDMA Band	824–890 MHz	−36 dBm to +36 dBm	Energy Scavenging
GSM 900 Band (UL)	890–915 MHz	±(5 dBm to 39 dBm)	Energy Scavenging
GSM 900 Band (DL)	935–960 MHz	±(5 dBm to 39 dBm)	Energy Scavenging
GPS	1575 ± 10 MHz	——	——
GSM 1800 Band (UL)	1710–1780 MHz	±(2 dBm to 36 dBm)	Energy Scavenging
GSM 1800 Band (DL)	1810–1900 MHz	±(2 dBm to 36 dBm)	Energy Scavenging
3G (Band-I)	1920–1980 MHz	±(2 dBm to 33 dBm)	Energy Scavenging
3G (Band-II)	2110–2170 MHz	±(2 dBm to 33 dBm)	Energy Scavenging
4G (LTE/LTE-A)	2300–2400 MHz	−36 dBm to +36 dBm	Energy Scavenging
Wi-Fi Band	2400 MHz	−36 dBm to +36 dBm	Energy Scavenging
Bluetooth Band	2450 MHz	−36 dBm to +36 dBm	Energy Scavenging
ISM Band	2400–2484 MHz	−36 dBm to +36 dBm	Energy Scavenging
ISM Band	2400 MHz	−36 dBm to +36 dBm	Energy Scavenging
WiMAX	3300–3700 MHz	−30 dBm to +30 dBm	Energy Scavenging
ISM Band	3600 MHz	−30 dBm to +30 dBm	Energy Scavenging
ISM Band	5000 MHz	−41 dBm to +41 dBm	Energy Scavenging
ISM Band	5200 MHz	−41 dBm to +41 dBm	Energy Scavenging
IEEE 802.11	5500 MHz	−41 dBm to +41 dBm	Energy Scavenging
IEEE 802.11	5800 MHz	−41 dBm to +41 dBm	Energy Scavenging
WLAN (LOWER)	5150–5725 MHz	−41 dBm to +41 dBm	Energy Scavenging
WLAN (UPPER)	5725–5875 MHz	−41 dBm to +41 dBm	Energy Scavenging

Of the great variety of available CP antenna systems, it has gained wide and tremendous popularity due to the ever-growing trend in the areas of system integration toward performance improvement in the wireless applications. Their modeling and attainment of low-profile features of the RF front-ends have been the subject of extensive research, which will always remain a great technical challenge and for which counter-related issues still need to be resolved with a new design (including a feasible solution). So, despite the progressive developments made in deploying the RF front-ends, there is still room for improvement in terms of the following characteristics (i.e., prerequisites of RF front-ends for maximizing outcomes from the application perspective) [11].

Due to such types of characteristics, these printed monopole antennas (PMAs) are usually used for the UWB bands (3.1-to-10.6 GHz). However, its implementation in the sub-6 GHz frequency bands (1-to-6 GHz) is quite restricted in number. On the contrary, their limited presence and its failure to achieve viability due to their non-responsive behavior towards CP characteristics (3 dB axial ratio bandwidth + CP gain) are one of the main limitations of printed monopole antennas. The technology itself suggests that an effective RF front-end is vastly required for implementing the design philosophy from an application perspective (primary objective) [12–17].

Here, the comprehensive analysis carried out in this review paper will focus on the realization and understanding of its current trends and the challenges of reconfigurable antennas from a design perspective. In addition, understanding the frequency of operation, the performance of antenna metrics: -10 dB impedance bandwidth (IBW), 3 dB axial ratio bandwidth (ARBW), antenna gain, antenna efficiency, and radiation pattern attributes are quite significant. Further, issues such as the transition from LP to CP, the attainment of a directional pattern, and scrutinizing trade-offs before going for the optimal solution are needed from an application point of view. Hence, along with the comprehensive review, a feasible solution has been provided that, to an extent, minimizes the system complexity and solves the limitation of designing reconfigurable antennas. The main highlights are as follows:

1. Reviewing the considerations of RF energy harvesting, analyzing its potential utilization of ambient RF signals, and addressing the growing presence of IoT, WSNs, and RFIDs.
2. Proposing and investigating a metasurface reflector-based CP reconfigurable antenna, aiming to advance the practical implementation of efficient RF energy harvesting systems.
3. Evaluating the RF energy harvesting capability through integration with the GVD rectifier circuit. Theoretical analogies are derived for parameters such as RF-to-DC power conversion efficiency ($\eta_{\circ}$, %) and DC harvested voltage (V_{out}, V) to assess system performance.
4. Presenting a theoretical framework for demonstrating circular polarization (CP) and emphasizing the importance of finding a DC biasing mechanism for polarization reconfigurability, particularly the dynamic switching from LP to CP.

In light of the proposed solution from the design perspective, a circularly polarized printed monopole antenna (CP-PMA) inspired by the incorporation of metasurfaces (MS) in the form of a reflector is proposed for the RF-EH application [11]. Since the primary source of input are EM waves coming out in the form of ambient RF signals from the various wireless communication bands (i.e., mostly in the sub-6 GHz frequency bands), microwave antennas are considered an intrinsic part of the RF-EH system. So, its practical realization and consideration of the performance trade-offs, such as the achievement of enhanced CP characteristics, broadened bandwidth responses (IBW/ARBW), high CP antenna gain, consistent antenna efficiency, and a directional radiation pattern with the good boresight strength at both principal planes, are so significant in nature [11]. Before delving into the design aspects of an efficient RF-EH system, a unified understanding and exploration of cutting-edge RF front-ends must be reviewed, with an eye to the usage of diodes (number), complexity of DC biasing circuits, and the attainment of polarization reconfigurability. Because, the trade-offs for usage of diodes and complexity of DC biasing circuit gives an overall idea about the performances regarding the attainment of polarization reconfigurability.

2. Reconfigurable Antennas and Their Usage in RF Energy Harvesting Application

In order to balance the trade-offs [7], microwave antennas are the top-most priority. They are classified as dipole antennas [18–21], monopole antennas [22–25], loop antennas [26–29], slot antennas [30–33], microstrip antennas [34–37], Vivaldi antennas [38–41], and DRAs [42–45]. Further, the classification is divided into helical antennas [46–49], Yagi–Uda antennas [50–53], and log-periodic antennas [54–57]. Depending upon the applied implicit techniques, their categorization is continued based upon the high-performance antennas [58–61], metamaterial/metasurface antennas [62–65], circularly polarized antennas [66–69], and array antennas [70–73].

The advanced feature of these reconfigurable antennas is the maximization of wireless communication through the integration of many radios onto a single platform. Due to their ability to operate over a broad frequency range, modify their geometries, and adapt to changes, reconfigurable antennas are therefore being viewed as a practical solution to cover the variety of wireless services [74–77]. There are several reconfiguration properties: frequency reconfigurability [78–81], polarization reconfigurability [82–85], pattern reconfigurability [86–89], hybrid reconfigurability [90–93], electrical diversity [94–97], optical diversity [98–101], mechanical diversity [102–105], material diversity [106–109], etc.

Subsequently, a comparative focus with its concurrent analysis on the reconfigurable antennas in RF energy harvesting [110–139] is explored. Furthermore, microwave antenna characteristics consist of (a) frequency of operation; (b) antenna gain, with the RF energy harvesting properties, including (c) RF-DC power conversion efficiency; and (d) DC output voltage. Technically, reconfigurable antenna at LTE (3.5 GHz), Wi-Fi (5 GHz), WiMAX (3.5–5.5 GHz), ISM (5 GHz), 5G (5 GHz), n77 (3.3–4.2 GHz), n78 (3.3–3.8 GHz), LTE Band 46 (5.15–5.85 GHz), and WLAN (IEEE 802.11 b/g/n) are incorporated with a metasurface (MS) reflector and integrated with the GVD rectifier circuit. It is designed, simulated, and investigated by using the CST microwave studio suite (EM simulation part) and ADS solver (circuit part). Furthermore, the results obtained from our investigation are in accordance with the attainment of trade-offs such as broadband circular polarization (CP), high antenna gain, consistent antenna efficiency, and lesser structure complexity, due to the elimination of extra biasing circuits. Finally, on execution, it can generate a DC harvested voltage (V_{out}) of around 5.8 volts and the RF-to-DC power conversion efficiency of up to 75% with the integration of the GVD rectifier circuit.

Thereby, the proposed metasurface (MS) antenna exhibits improved 3 dB axial ratio bandwidth and CP antenna gain. Most importantly, the existing antenna trade-offs, i.e., usage of diodes (number), complexity of DC biasing circuits, and the attainment of polarization reconfigurability) in the same field of interest are resolved. Adding more into it, the number of diodes used in the previous case is two or more, which literally adds congestion through the incorporation of additional DC biasing circuits. Due to this, the attainment of polarization reconfigurability could not be achieved to its maximum extent, looking from the application perspective.

A comparative focus on this ground, along with its state-of-the-art references, is highlighted in Table 2 and Figures 2–5, respectively. In the next section, the complete design perspective of a reflector-inspired CP-based reconfigurable antenna is presented, along with its corresponding outcomes. It will act as a generic solution for improving the state transition for reconfigurability [140], aimed at addressing the requirements of various wireless applications. It is also observed that, for the selection of a reconfiguration technique, there is a dependency on the property of reconfigurable antenna geometry. That is why an antenna designer selects the technique in such a way that it satisfies generic imposed constraints and at the same time and completes the antenna designing process very efficiently.

Table 2. Comparison of reconfigurable antennas used in RF energy harvesting application [110–139].

References	Operating Band	Antenna Gain	η_o	V_{out}
[110]	WLAN	5.7 dBi	43%	1.5 V
[111]	WLAN	6.7 dBi	71%	——
[112]	WLAN	4.5 dBi	55.1%	——
[113]	ISM	4 dBi	65.3%	3.2 V
[114]	WLAN	——	——	4.9 V
[115]	WLAN	5.68 dBi	50.2%	1.2 V
[116]	ISM	——	69.1%	——
[117]	ISM	——	37.8%	2.76 V
[118]	ISM	——	47%	0.43 V
[119]	5.6 GHz	7.6 dBi	43%	2.1 V
[120]	ISM	8 dBi	82.3%	——
[121]	ISM	7.5 dBi	61%	——
[122]	915 MHz	3.8 dBi	88.5%	4.6 V
[123]	5.8 GHz	6.38 dBi	76%	——
[124]	915 MHz	1.6 dBi	18%	2 V
[125]	ISM	2.84 dBi	35.5–52.2%	——
[126]	ISM	5 dBi	70.2%	4 V
[127]	ISM	——	75.5%	5.21 V
[128]	ISM	——	41.63%	——
[129]	ISM	2.19 dBi	65%	2.6 V
[130]	UWB	15 dBi	——	——
[131]	ISM	5.9 dBi	55.3%	3.3 V
[132]	ISM	——	79%	4.13 V
[133]	ISM	6.4 dBi	74%	2.9 V
[134]	UWB	2.1–4.3 dBi	——	——
[135]	WLAN	8.6 dBi	57.3%	1.74 V
[136]	ISM	1.94 dBi	——	——
[137]	1.8/5.2 GHz	4.5 dBi	——	——
[138]	2.8 GHz	2–8 dBi	10–80%	7 V
[139]	ISM	6.8 dBi	63%	2.82 V

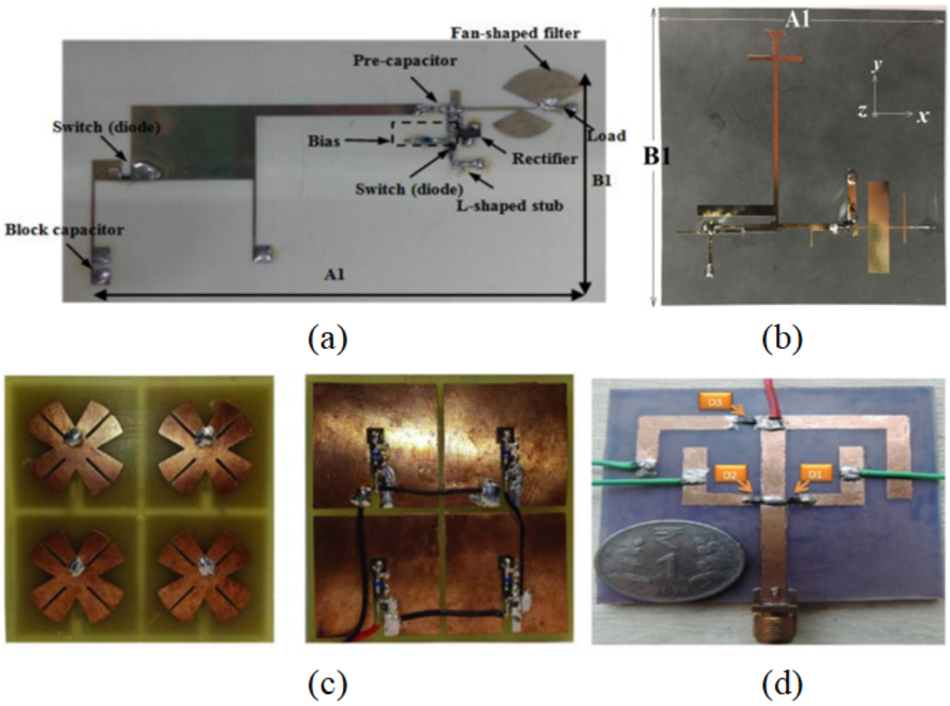

Figure 2. Overview of the frequency reconfigurability antennas for RF energy harvesting applications (**a**) [111], (**b**) [112], (**c**) [113], and (**d**) [114].

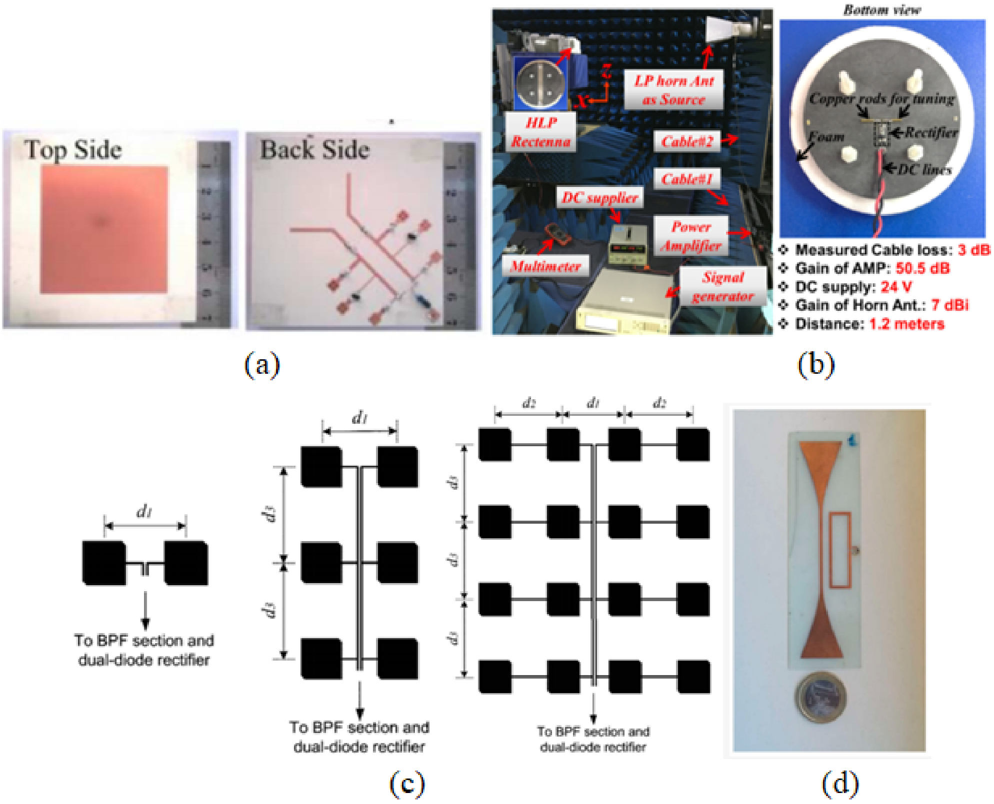

Figure 3. Overview of the polarization reconfigurability antennas for RF energy harvesting applications (**a**) [121], (**b**) [122], (**c**) [123], and (**d**) [124].

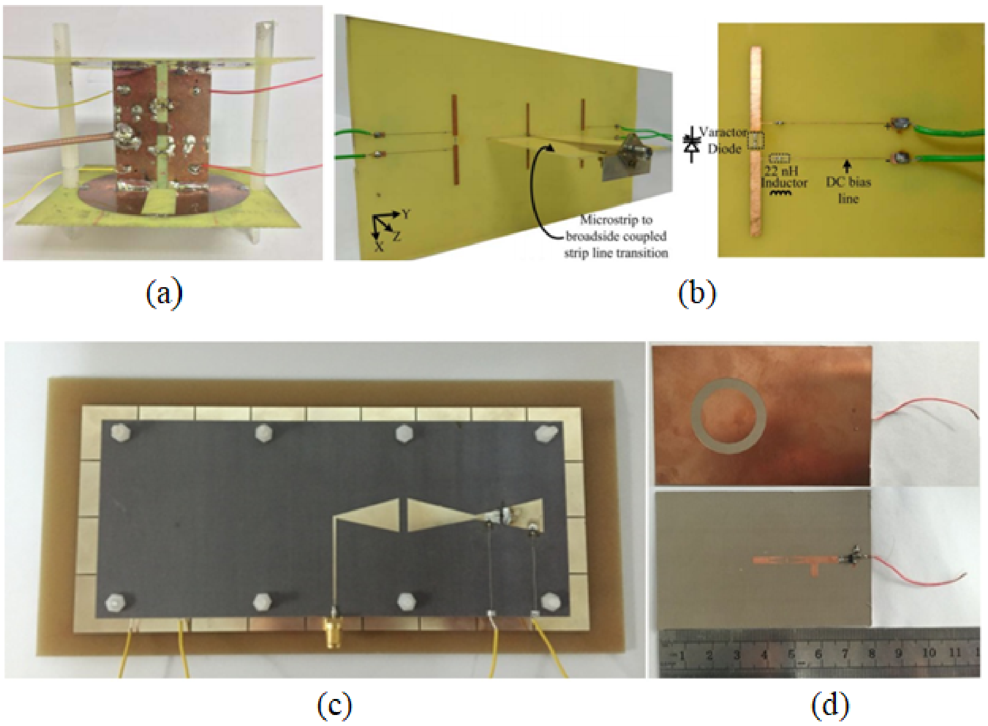

Figure 4. Overview of the pattern reconfigurability antennas for RF energy harvesting applications (**a**) [87], (**b**) [88], (**c**) [140], and (**d**) [126].

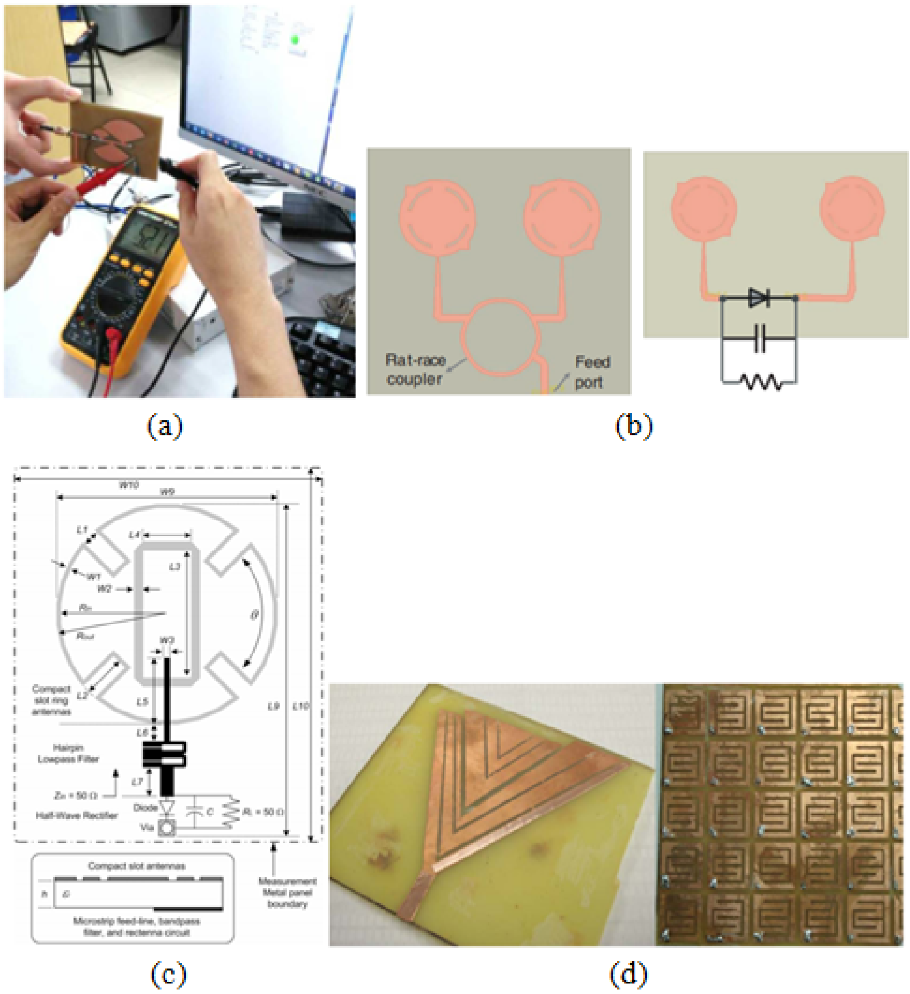

Figure 5. Overview of the hybrid (combination of frequency, polarization, or pattern) reconfigurability antennas for RF energy harvesting applications (**a**) [127], (**b**) [128], (**c**) [129], and (**d**) [130].

3. Case Study: Solution from Design Perspective

In this section, the metasurface reflector-based CP reconfigurable antenna integrated with a rectifier is taken as a case study and investigated for the RF energy harvesting. It illustrates the achievement of design trade-offs such as broad 3 dB axial ratio bandwidth, higher antenna gain, consistent antenna efficiency, and a directional pattern with a wider 3 dB angular beamwidth [11]. Along with the realization of this reconfigurable antenna, a proper understanding of emission power levels at various frequencies is needed, as shown in the Table 1. These reconfigurable antennas presented in Table 2 have used two or more diodes for their operation. The presence of a larger number of diodes increases the circuit complexity. Additionaly, the coverage for antennas in the sub-6 GHz band is found to be limited. So, a more practical solution needs to be realized, as briefed earlier in the previous section.

Thus, a metasurface reflector-inspired reconfigurable broadband circularly polarized Y-shaped monopole antenna is proposed for the 3.5/5 GHz bands. Here, it consists of a Y-shaped radiating monopole and a 50 Ω microstrip feed line for input excitation. The traditional monopole antenna with a partial ground plane is limited in its ability to achieve polarization and pattern attributes. Therefore, the partial ground plane is shorted with a parasitic conducting strip (PCS_L) by using a BAR 50-02V RF PIN diode from Infineon Technologies. It is capable of generating the horizontal and vertical components required to witness the existence of CP fields. Such an occurrence of events is often confirmed by surface current distribution, electric field distribution, and a far-field radiation pattern [11].

To meet the trade-offs, a metasurface (MS) reflector is placed just below the Y-shaped radiator at an air gap of 20 mm. As a result, the 3 dB axial ratio bandwidth is improved from 460 MHz to 1.23 GHz (a rise of 3.08 times) with an enhancement of CP antenna gain from 3.6 dBic to 8.45 dBic (a rise of 2.35 times). Hence, for the RF-to-DC conversion, a multi-stage GVD rectifier is incorporated. The RF-to-DC conversion efficiency (η_o, %) is calculated on the basis of Equation (1). Here, the DC output voltage (V_{out}) is greater than 4.8 volts, with an RF-to-DC conversion efficiency of greater than 55% at 12 dBm across the operating frequency bands. Their detailed behavioral insights are shown in Figure 6a–d and Table 3, respectively.

$$\eta_0(\%) = \frac{P_{\text{load}}}{P_{\text{incident}}} = \frac{V^2{}_{\text{out}}}{P_{\text{in}} \times R_{\text{load}}} \tag{1}$$

Besides implementing the CP RF front-ends (CP-PMAs), detailed theoretical insights are presented for understanding the different behavioral aspects in hope of understanding the existence and behavior of CP for PMAs, the placement of reflectors below radiating structures, performance analysis related to the enhancement of IBW and ARBW, enhanced CP antenna gain, and attainment of directional patterns with improved front-to-back ratio (FBR) for the MS. As a result, the proposed contribution includes the achievement of performance trade-offs. In the end, the usage of a PIN diode (BAR 50-02 V) from Infineon Technologies with a simple biasing circuit is reported, which minimizes the overall complexity of the system by alleviating the use of additional DC biasing circuits.

Table 3. The performance metrics of polarization reconfigurable printed monopole antenna with the metasurface reflector, integrated with a multi-stage rectifier circuit. (Notations: LP—linearly polarized, CP—circularly polarized, and HPBW—half-power beamwidth).

Parameters	Stage-1	Stage-2	Stage-3	Stage-4
Geometry Traits	Initial	OFF-State	ON-State	Final
Polarization	LP	LP	CP	CP
IBW	830 MHz	620 MHz	2.11 GHz	2.38 GHz
ARBW	——	——	460 MHz	1.23 GHz
HPBW	——	——	60°	>110°
Antenna Gain	2.3 dBi	2.4 dBi	3.6 dBic	>8.35 dBic
η_o	——	——	——	>55% @12 dBm
V_{out}	——	——	——	>4.8 V @12 dBm

In the next section, an analogy about the theoretical aspects of CP backed by surface current distribution, the study of electric field pattern in the context of the plane wave equation, and correlation with a Cartesian plot of the far-field normalized pattern is highlighted with respect to the proposed antenna. With insights into DC biasing mechanisms, the intuitions behind the attainment of directional radiation pattern characteristics are also presented as a generic solution to the observed limitations.

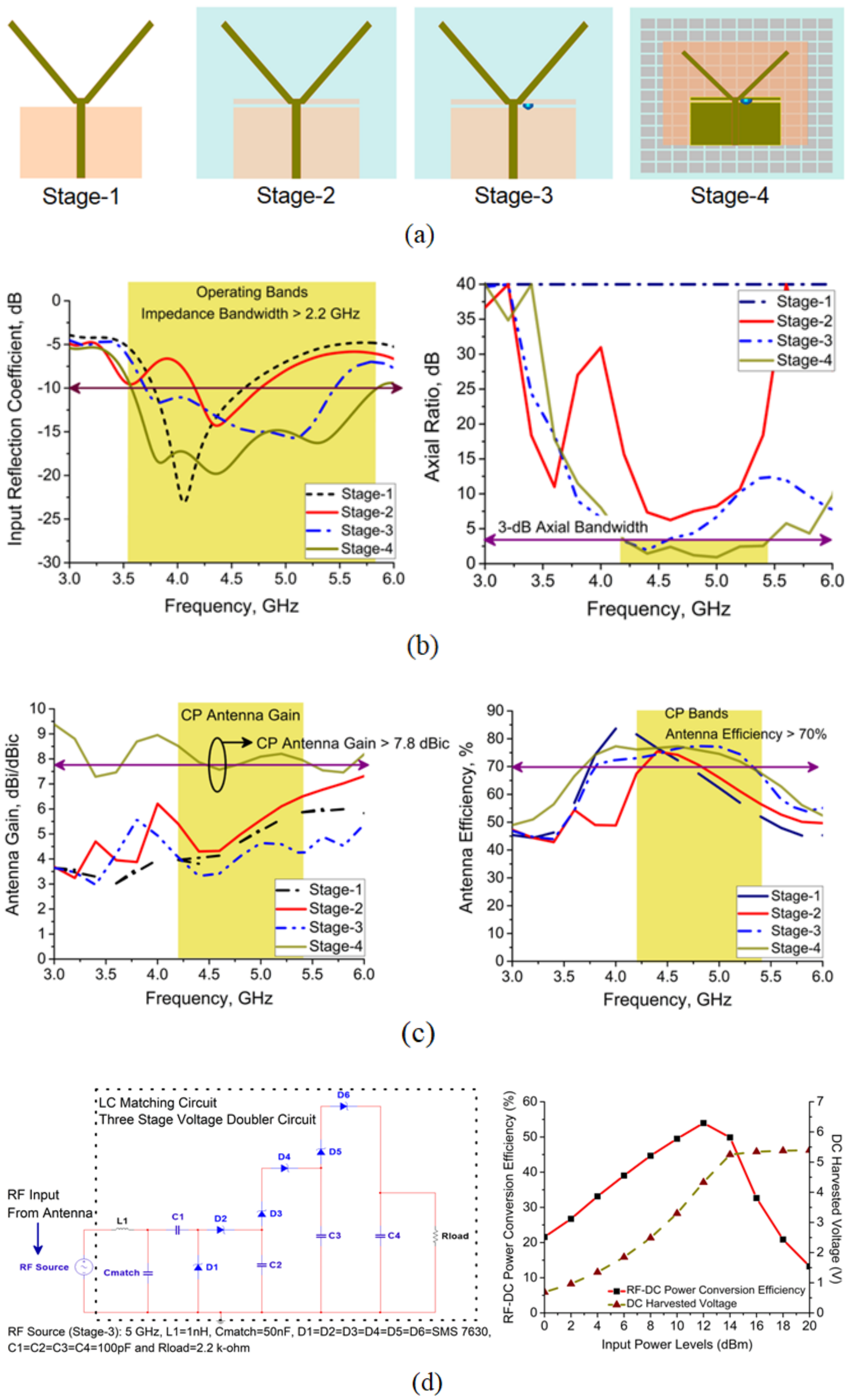

Figure 6. (**a**) Schematic configuration and evaluation of metrics such as the (**b**) −10 dB impedance bandwidth (IBW) and 3 dB axial ratio bandwidth (ARBW), (**c**) antenna gain and antenna efficiency, and (**d**) RF-to-DC conversion efficiency (η_o) and DC harvested voltage (V_{out}). So, the developmental steps of the proposed antenna are as follows. Stage-1 (initial): Y-shaped printed monopole antenna + partial ground. Stage-2: Y-shaped printed monopole antenna + partial ground + PCS_L + Diode-OFF state. Stage-3: Y-shaped printed monopole antenna + partial ground + PCS_L + Diode-ON state. Stage-4 (final): Y-shaped printed monopole antenna + partial ground + PCS_L + Diode-ON state + metasurface reflector (PYMA-MS).

4. Insights

The outcomes depicted by the aforesaid metasurface (MS) antenna are more effective than their counterparts reported in [1–17]. It witnesses good impedance matching over the desired frequency bands and is a feasible solution for achieving the trade-offs such as broadband circular polarization (CP), higher antenna gain, consistent antenna efficiency, single diode usage, and a directional radiation pattern with a wide 3 dB angular beamwidth of 110°–130° at f = 4.5 GHz. In order to understand the physical insights, different studies are presented below.

1. Phenomenon-A: Transition from LP-to-CP characteristics.
2. Phenomenon-B: Intuition behind the implementation of metasurface reflector.
3. Phenomenon-C: Understanding the DC biasing mechanism toward reconfigurability.
4. Phenomenon-D: Exploration for RF energy harvesting as a prospective application.

4.1. Transition from LP-to-CP

For a better understanding of circular polarization (CP) characteristics, the axial ratio (AR $\leq$ 3 dB) is considered the primary indicator. Here, CP analysis is backed by (a) surface current distribution, (b) electric field distribution, along with its theoretical insights with respect to the plane waves and its modeling with relationship to the far-field observables, and (c) a normalized radiation pattern, can be seen in Figure 7a–d, respectively.

The first primitive approach to analyzing CP is through the surface current distribution. At stage-2, due to the absence of parasitic conducting strips (PCS), no connection is established with the partial ground plane. Induced surface currents on the horizontal edges of the partial ground plane are found in the opposite direction, canceling each other out and leaving only the vertical surface currents on the monopole arm. Hence, a linearly polarized (LP) wave is generated (OFF-state). In stage-3, when one of the parasitic conducting strips (PCS_L) is shorted with the partial ground plane, through a BAR50-02V PIN Diode from Infineon Technologies, the surface currents on PCS_L and partial ground plane are rearranged in such way that the resultant currents on the upper edge of PCS_L and the lower edge of the partial ground plane do appear in the same direction, inducing out horizontal surface currents. The presence of both horizontal (x) and vertical (y) components in terms of horizontal and vertical currents leads to the generation of CP characteristics (ON-state).

The second primitive approach to analyzing CP is through electric field distribution. When PCS_L is connected to partial ground plane through the BAR50-02V PIN Diode, the CP reconfigurable antenna realizes LHCP in the +z direction (i.e., outward in nature). The rotation of electric field vectors changes in a clockwise direction, with a change in the phase from 0° to 90° at f = 4.5 GHz. Therefore, an orthogonal change in the electric field pattern confirms the generation of left-handed circularly polarized waves (LHCP).

The third primitive approach to analyzing CP is through normalized radiation pattern. It correlates with the relative power from the normalized radiation pattern (i.e., the cartesian plot) at f = 4.5 GHz. In the broadside direction, the antenna has excellent LHCP characteristics. The LHCP is stronger than the RHCP by -21 dBic in their desired bands.

The explanations of circular polarization (CP) have been explored using the following approaches: I, II, and III. It is related to the analysis of transverse components in that far-field observations are frequently treated as far-field vector components, which correspond significantly to the polarization varsities, i.e., the linear, circular, or elliptical, respectively.

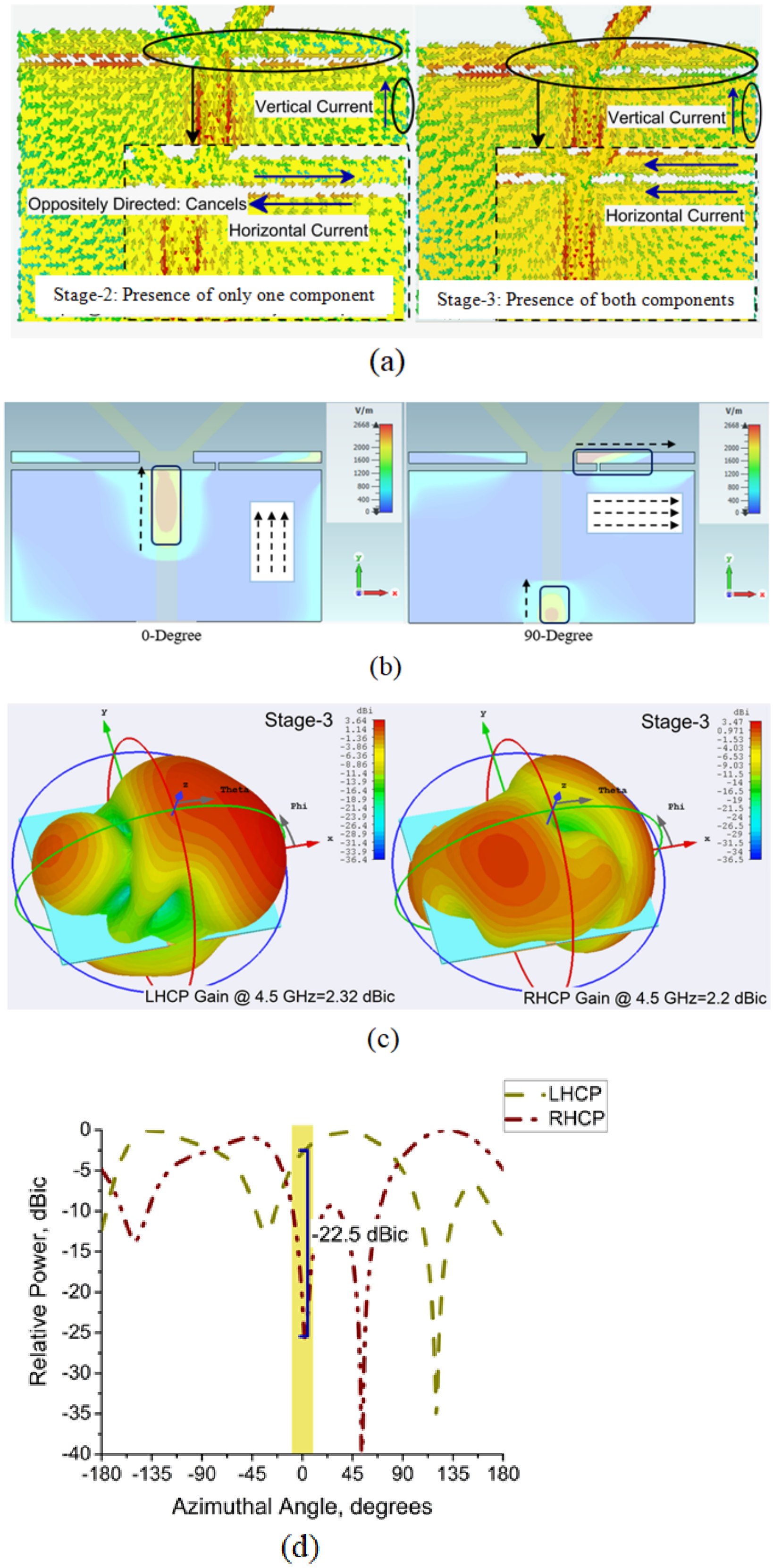

Figure 7. Analysis of CP mechanism of the proposed polarization reconfigurable metasurface-inspired printed monopole antenna. (**a**) Approach-I, (**b**) Approach-II, (**c**,**d**) Approach-III at f = 4.5 GHz.

4.2. Intuition Behind Implementation of Metasurface Reflector

The design and development of a metasurface reflector are investigated in this case by evenly dividing the entire rectangular patch of $1.78\lambda_{\circ} \times 1.48\lambda_{\circ}$ into grid-slotted sub patches of 12×12 cells, with each cell of being $0.13\lambda_{\circ} \times 0.009\lambda_{\circ}$ and an intermediate gap of 1 mm between them. As a consequence, TM_{10} mode is found on each sub-patch that contributes towards the generation of quasi-TM_{30} mode. The presence of such higher-order modes frequently results in a broadened impedance and 3 dB axial ratio bandwidth [141,142]. When the metasurface reflector comes into contact with the radiator, it redirects out one-half of the radiated waves in the opposite direction and partially shields objects on the other side. Such behavior is seen due to radiated waves from a reflector-based printed monopole antenna that consist of (a) directed waves from the Y-shaped monopole radiator and (b) reflected waves from the metasurface reflector. It exhibits a directional radiation property, as shown in the Figures 8–10. In addition to it, the average CP antenna gain is enhanced by 2.35 times, the 3 dB axial ratio bandwidth is also improved with a rise of 3.08 times, and a fractional bandwidth of >25% is attained. Thus, the changes in this type of characteristic are often attributed to the movement of incoming currents and the generation of stronger orthogonal fields over the desired CP frequency bands [143–148].

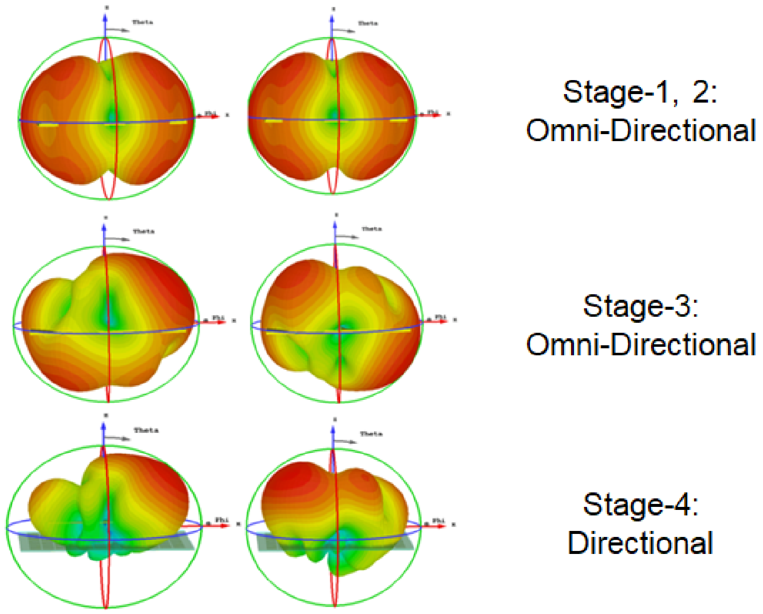

Figure 8. Transition of pattern behavior from omni-directional to directional due to the implementation of metasurface (MS).

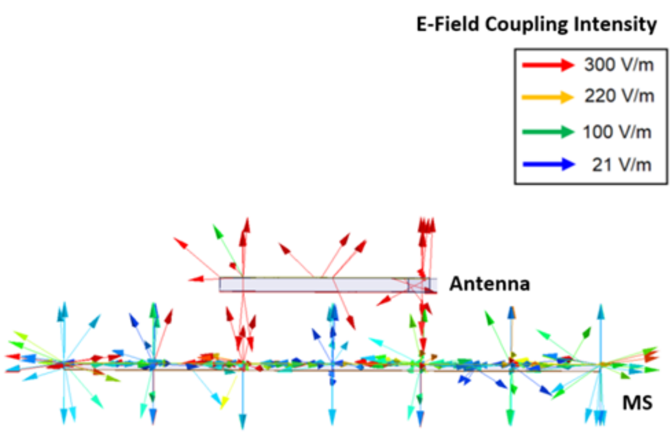

Figure 9. Coupling process of proposed antenna configuration loaded with metasurface reflector.

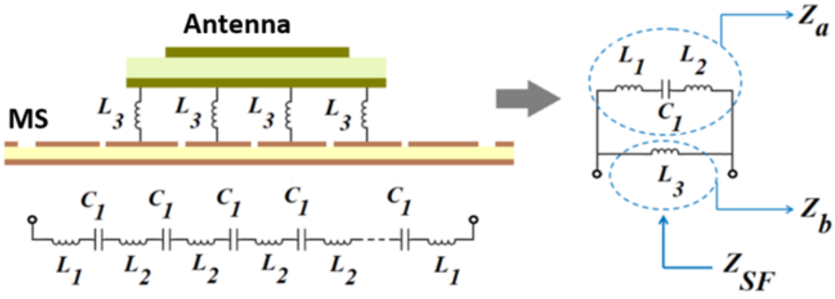

Figure 10. Equivalent circuit model of metasurface reflector loaded under monopole antenna.

4.3. Understanding DC Biasing Mechanism

By connecting an extended partial ground plane and one of the parasitic conducting strips with the aid of a single BAR 50-02V PIN Diode (ON-state) from Infineon, polarization reconfigurability is achieved. So, the equivalent of an Infineon BAR 50-02V PIN Diode is simulated in the CST microwave studio with a 3Ω forward resistance in the ON-state and a 5 kΩ reverse parallel resistance with 0.15 pF reverse parallel capacitance in the OFF-state. Here, the forward current of the 18 mA forward input voltage of 1 V is measured, with 0.89 V as the voltage drop across the PIN diode as the extended partial ground plane is connected to the BAR 50-02V PIN Diode in this instance. Thus, a minimal loss is introduced in this proposed antenna, which reduces complexity at the time of practical realization shown in Figures 11–14.

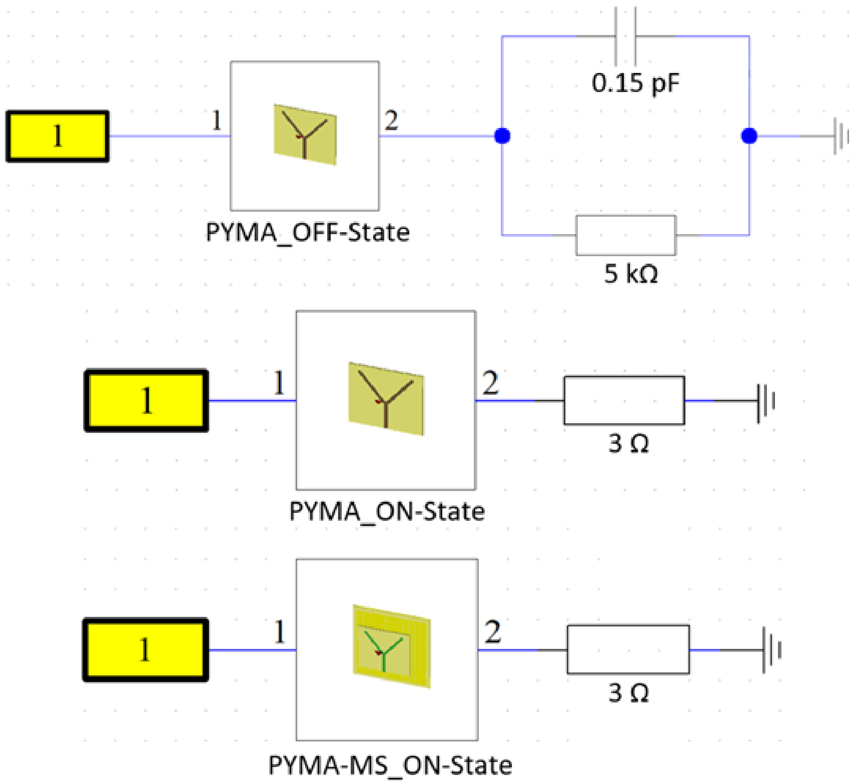

Figure 11. Biasing configuration setup of the polarization reconfigurable printed monopole antenna in CST microwave suite.

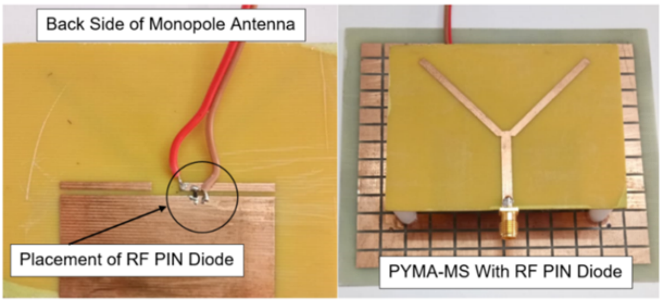

Figure 12. Fabricated prototype of the polarization reconfigurable printed monopole antenna loaded with metasurface reflector.

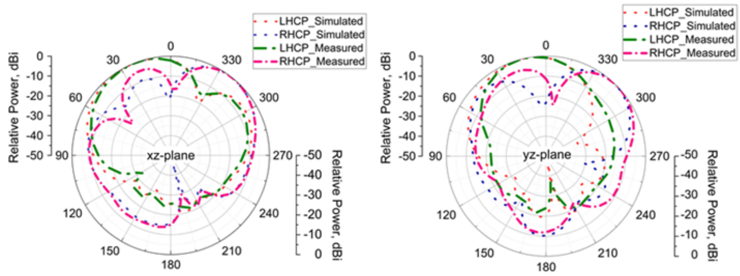

(a)

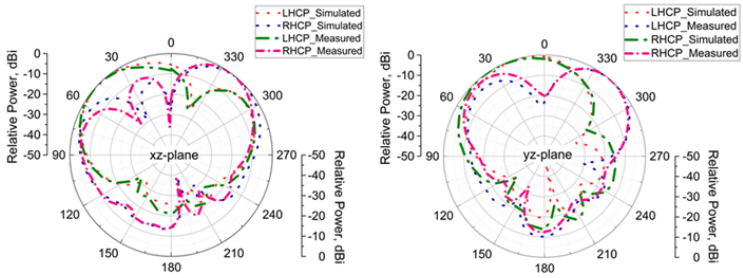

(b)

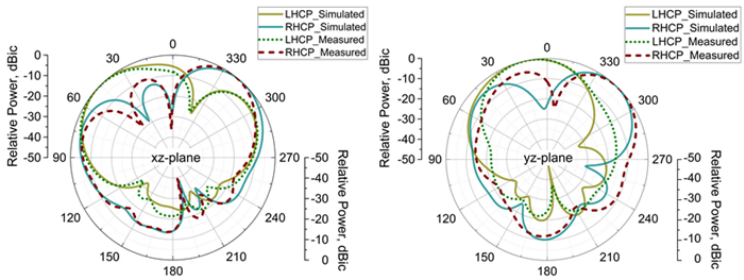

(c)

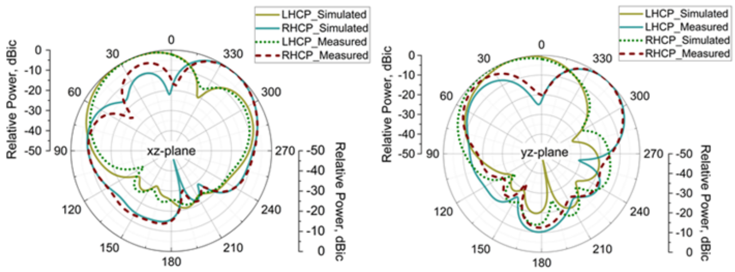

(d)

Figure 13. Patterns at (**a**) 4.5 GHz (OFF), (**b**) 4.5 GHz (ON), (**c**) 5 GHz (OFF), and (**d**) 5 GHz (ON).

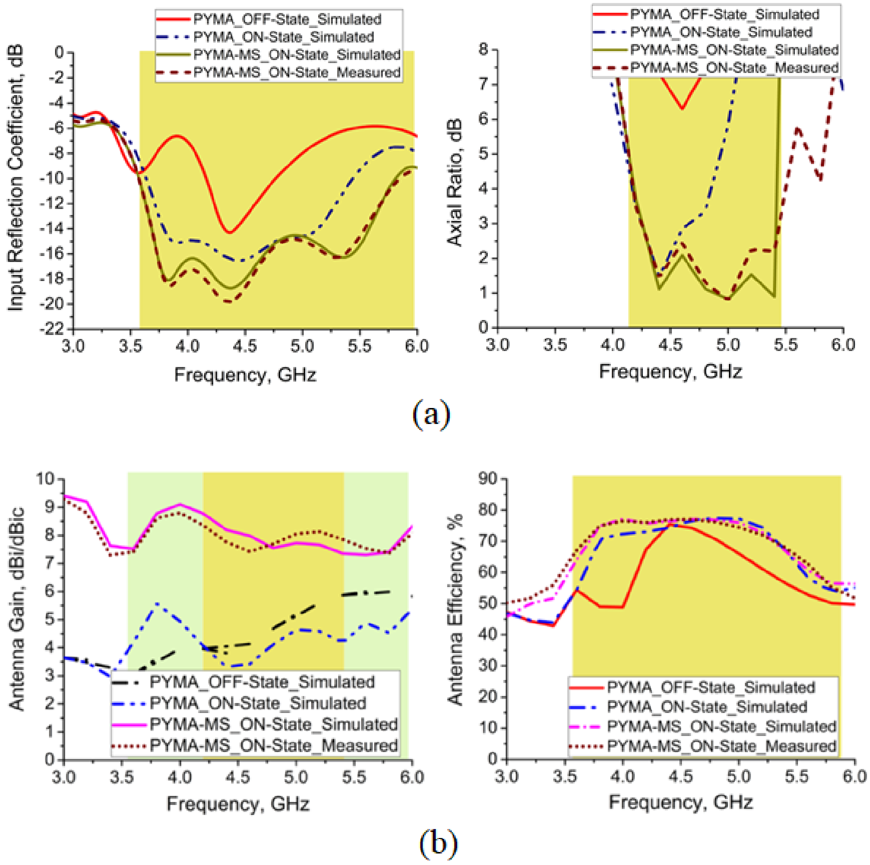

Figure 14. Validated metrics such as (**a**) IBW and ARBW and (**b**) antenna gain and antenna efficiency.

4.4. RF Energy Harvesting: Prospective Application

For incorporating the phenomenon of RF energy harvesting into the real-time aspect, there is a need to convert these ambient RF signals into a DC output, for which highly efficient and wideband rectifier circuits (GVDs) are required and need to be appended with the impedance matching network (IMN) to the CP RF front-ends. Henceforth, the viability of the entire system significantly depends depending on the performance of these individual units [RF front ends (antennas) + impedance matching network (IMN) + rectifier circuits (GVDs)]. Thereby, the overall working idea remains with the development of an extensive system that fulfills the increasing power requirements to carry out the robust operations of the multi-functional electronic components for both consumer and commercial usage, provided that the proposed RF front-ends are able to achieve the performance trade-offs before integrating them with the proposed rectifier circuits. To satisfy these types of needs, the design and implementation of CP-printed monopole antenna (CP-PMAs) operating in the sub-6 GHz frequency bands with enhanced performance due to incorporation of metasurfaces (MS) embedded with the multi-stage rectifier circuit systems (GVDs) being thought to be very important in terms of performance trade-offs [12]. Furthermore, the entire scenario (Y-shaped monopole antenna + metasurface reflector) is represented by Equations (2) and (3). Therefore, the overall results resulted in the powering of sensors found in low-power devices (such as wearables, and medical and healthcare plug-based kits), which require a constant DC output voltage of around 2.4–5.5 V to operate. In short, this particular technology will gradually play a crucial role in designing efficient systems. Although it faces so many issues, overcoming these challenges gives rise to an era of clean, green, and sustainable energy for the 5G/6G [149–155] applications of recent times.

$$f_R = \frac{j\omega L_3(1 - \omega^2 L_1 C_1 - \omega^2 L_2 C_1)}{1 - \omega^2 L_1 C_1 - \omega^2 L_2 C_1 - \omega^2 L_3 C_1} \quad (2)$$

$$h_{\text{air-gap}} = 0.36\lambda_{5\,GHz} - h_{\text{sub}}\sqrt{\varepsilon_{\text{r}}} \quad (3)$$

In a practical testing scenario of the polarization reconfigurable mechanism electronically, the BAR50-02V PIN RF Diode as a switch from Infineon with package P-SC79-2-1 is used. The voltage conditions are applied for ON-state (forward voltage, V_F = 0.95 V) and for OFF-state (reverse voltage, V_R = 50 V) when applied to the RF PIN diode through the DC power supply. From the radiation graphs shown, LHCP and RHCP are isolated by >15.5 dBic (simulated) and >25.2 dBic (measured) indicating that the LHCP is dominant as compared to RHCP with front-to-back ratio (FBR) ranging from −15 dBic to −23.5 dBic, as shown in Figure 13.

5. Conclusions

This review article presents a comprehensive summary of the recent advancements in reconfigurable antenna technology for RF energy harvesting. Since electromagnetic waves constitute the main input, microwave antennas are regarded as an integral component of the RF energy harvesting system. Thus, it is important to address its practical realization and trade-offs. However, before beginning the designing process, it is necessary to have a thorough understanding of the principles of RF transmission, insights into rectification behavior, and an investigation of reconfigurable antennas in RF energy harvesting. At first, a wideband, CP, reconfigurable Y-shaped monopole antenna is reported. Conventional antennas were unable to accomplish trade-offs. Improvements in IBW, ARBW, CP antenna gain, antenna efficiency, and attainment of the directional pattern are seen in the case study with the addition of the metasurface reflector. In addition, the conditions such as usage of diodes (number), the complexity of DC biasing circuits, and the attainment of polarization reconfigurability are also taken care of. The three-stage Greinacher voltage doubler and LC matching (IMN) rectifier circuit are integrated into the metasurface reflector-inspired CP reconfigurable antenna (GVD). Here, the designed rectifier circuit is examined for input power levels (P_{in}) ranging from 0 to +20 dBm, V_{out} is of >4.86 V with the η_o as >55% at 12 dBm when simulating at the ADS platform with a load resistance (R_{load}) of 2.2 kΩ, which is quite enough to efficiently power the sensors in internet-of-things (IoT) and wireless sensor nodes (WSNs).

Author Contributions: Conceptualization, B.R.B. and S.K.M.; methodology, B.R.B. and S.K.M.; writing—original draft preparation, B.R.B. and S.K.M.; writing—review and editing, B.R.B., S.K.M., M.H.A. and A.J.; project administration, M.H.A., and A.J.; funding acquisition, M.H.A. and A.J. All authors have read and agreed to the published version of the manuscript.

Funding: This research received no external funding.

Institutional Review Board Statement: Not applicable.

Informed Consent Statement: Not applicable.

Data Availability Statement: Not applicable.

Conflicts of Interest: The authors declare no conflict of interest.

References

1. Valenta, C.R.; Durgin, G.D. Harvesting wireless power: Survey of energy-harvester conversion efficiency in far-field wireless power systems. *IEEE Microw. Mag.* **2014**, *15*, 108–120.
2. Lu, X.; Wang, P.; Niyato, D.; Kim, D.I.; Han, Z. Wireless networks with RF energy harvesting: A contemporary survey. *IEEE Commun. Surv. Tutor.* **2015**, *184*, 266–298. [CrossRef]
3. Soyata, T.; Copeland, L.; Heinzelman, W. RF energy harvesting for embedded systems: A survey of trade-offs and methodology. *IEEE Circuits Syst. Mag.* **2016**, *16*, 22–57. [CrossRef]
4. Tran, L.G.; Cha, H.K.; Park, W.T. RF power harvesting: A review on designing methodologies and applications. *Micro Nano Syst. Lett.* **2017**, *5*, 1–16. [CrossRef]
5. Alimenti, F.; Palazzi, V.; Mariotti, C.; Mezzanotte, P.; Correia, R.; Carvalho, N.B.; Roselli, L. Smart hardware for smart objects: Microwave electronic circuits to make objects smart. *IEEE Microw. Mag.* **2018**, *19*, 48–68. [CrossRef]

6. Divakaran, S.K.; Krishna, D.D.; Nasimuddin. RF energy harvesting systems: An overview and design issues. *Int. J. RF Microw. Comput.-Aided Eng.* **2019**, *29*, e21633. [CrossRef]
7. Behera, B.R.; Meher, P.R.; Mishra, S.K. Microwave antennas-An intrinsic part of RF energy harvesting systems: A contingent study about design methodologies and state-of-the-art technologies in current scenario. *Int. J. RF Microw. Comput.-Aided Eng.* **2020**, *30*, e22148. [CrossRef]
8. Surender, D.; Khan, T.; Talukdar, F.A.; De, A.; Antar, Y.M.; Freundorfer, A.P. Key components of rectenna system: A comprehensive survey. *IETE J. Res.* **2020**, *22*, 3379–3405. [CrossRef]
9. Surender, D.; Khan, T.; Talukdar, F.A.; Antar, Y.M. Rectenna design and development strategies for wireless applications: A review. *IEEE Antennas Propag. Mag.* **2021**, *64*, 16–29. [CrossRef]
10. Sherazi, H.H.R.; Zorbas, D.; O'Flynn, B. A comprehensive survey on RF energy harvesting: Applications and performance determinants. *Sensors* **2022**, *22*, 2990. [CrossRef]
11. Behera, B.R.; Mishra, S.K. A single-layered metasurface inspired broadband polarization reconfigurable printed monopole antenna for hybrid wireless applications. *AEUE-Int. J. Electron. Commun.* **2022**, *156*, 154405. [CrossRef]
12. Behera, B.R.; Mishra, S.K. Investigation of a high-gain and broadband circularly polarized monopole antenna for RF energy harvesting application. *Int. J. Microw. Wirel. Technol.* 2022, *first view*. [CrossRef]
13. Mohanty, A.; Behera, B.R.; Esselle, K.P.; Alsharif, M.H.; Jahid, A.; Mohsan, S.A.H. Investigation of a dual-layer metasurface-inspired fractal antenna with dual-polarized/-modes for 4G/5G applications. *Electronics* **2022**, *11*, 2371. [CrossRef]
14. Behera, B.R.; Meher, P.R.; Mishra, S.K. Metasurface superstrate inspired printed monopole antenna for RF energy harvesting application. *Prog. Electromagn. Res. C* **2021**, *110*, 119–133. [CrossRef]
15. Behera, B.R.; Srikanth, P.; Meher, P.R.; Mishra, S.K. A compact broadband circularly polarized printed monopole antenna using twin parasitic conducting strips and rectangular metasurface for RF energy harvesting application. *AEUE-Int. J. Electron. Commun.* **2020**, *120*, 153233. [CrossRef]
16. Sahu, N.K.; Mishra, S.K. Compact dual-band dual-polarized monopole antennas using via-free metasurfaces for off-body communications. *IEEE Antennas Wirel. Propag. Lett.* **2022**, *21*, 1358–1362. [CrossRef]
17. Sahu, N.K.; Mishra, S.K. Polarization converting metasurface inspired dual band dual circularly polarized monopole antennas for OFF body communications. *IEEE Antennas Wirel. Propag. Lett.* **2022**, *22*, 194–198. [CrossRef]
18. Xu, Y.; Guo, L.; Xue, W.; Vladimir, K.; Qi, J. An optimal electric dipole antenna model and its field propagation. *Int. J. Antennas Propag.* **2016**, *2016*, 8601497. [CrossRef]
19. Almoneef, T.S.; Sun, H.; Ramahi, O.M. A 3-D folded dipole antenna array for far-field electromagnetic energy transfer. *IEEE Antennas Wirel. Propag. Lett.* **2016**, *15*, 1406–1409. [CrossRef]
20. Sarma, S.S.; Akhtar, M.J. A dual band meandered printed dipole antenna for RF energy harvesting applications. In Proceedings of the 2016 IEEE 5th Asia-Pacific Conference on Antennas and Propagation, Kaohsiung, Taiwan, 26–29 July 2016; pp. 93–94.
21. Zeb, H.; Gohar, M.; Ali, M.; Rahman, A.U.; Ahmad, W.; Ghani, A.; Choi, J.-G.; Koh, S.-J. Zero energy IoT devices in smart cities using RF energy harvesting. *Electronics* **2023**, *12*, 148. [CrossRef]
22. Arrawatia, M.; Baghini, M.S.; Kumar, G. Broadband bent triangular omnidirectional antenna for RF energy harvesting. *IEEE Antennas Wirel. Propag. Lett.* **2016**, *15*, 36–39. [CrossRef]
23. Mathur, M.; Agarwal, A. A compact coplanar waveguide wideband monopole antenna for RF energy harvesting applications. *Prog. Electromagn. Res. M* **2018**, *63*, 175–184. [CrossRef]
24. Kurvey, M.; Kunte, A. Harvesting RF energy using slotted tri-stepped rectangular monopole antenna. *Wirel. Pers. Commun.* **2022**, *126*, 3465–3474. [CrossRef]
25. Prashad, L.; Mohanta, H.C.; Mohamed, H.G. A compact circular rectenna for RF-energy harvesting at ISM band. *Micromachines* **2023**, *14*, 825. [CrossRef]
26. Noguchi, A.; Arai, H. Small loop rectenna for RF energy harvesting. In Proceedings of the 2013 Asia-Pacific Microwave Conference Proceedings, Seoul, Republic of Korea, 5–8 November 2013; pp. 86–88.
27. Stoopman, M.; Keyrouz, S.; Visser, H.J.; Philips, K.; Serdijn, W.A. Co-design of CMOS rectifier & small loop antenna for highly sensitive RF energy harvesters. *IEEE J. Solid-State Circuits* **2014**, *49*, 622–634.
28. Mansour, M.; Sultan, K.; Kanaya, H. Compact dual-band tapered open-ended slot-loop antenna for energy harvesting systems. *Electronics* **2020**, *9*, 1394. [CrossRef]
29. Zeng, M.; Andrenko, A.S.; Liu, X.; Li, Z.; Tan, H.Z. A compact fractal loop rectenna for RF energy harvesting. *IEEE Antennas Wirel. Propag. Lett.* **2017**, *16*, 2424–2427. [CrossRef]
30. Nakano, H.; Yamauchi, Y. Printed slot and wire antennas: A review. *Proc. IEEE* **2012**, *100*, 2158–2168. [CrossRef]
31. Shastri, A.; Jun, S.; Sanz-Izquierdo, B.; Aldawas, H.; Ahmed, Q.; Sobhy, M. Evaluation of low-cost inkjet printed slot antenna for energy harvesting applications. In Proceedings of the 2016 Loughborough Antennas & Propagation Conference, Loughborough, UK, 14–15 November 2016; pp. 1–5.
32. Chen, W.-S.; Cheng, C.-M.; Liao, B-Y.; Chang, Y.-L.; Wang, H.-Y. Triple-band slot antenna array for energy harvesting for wireless sensor networks. *Sensors Mater.* **2018**, *30*, 584–594. [CrossRef]
33. Muhammad, S.; Smida, A.; Waly, M.I.; Mallat, N.K.; Iqbal, A.; Khan, S.R.; Alibakhshikenari, M. Design of wideband circular-slot antenna for harvesting RF energy. *Int. J. Antennas Propag.* **2022**, *2022*, 5964753. [CrossRef]

34. Boursianis, A.D.; Papadopoulou, M.S.; Koulouridis, S.; Rocca, P.; Georgiadis, A.; Tentzeris, M.M.; Goudos, S.K. Triple-band single-layer rectenna for outdoor RF energy harvesting applications. *Sensors* **2021**, *21*, 3460. [CrossRef]
35. Arrawatia, M.S.; Baghini, M.S.; Kumar, G. Differential microstrip antenna for RF energy harvesting. *IEEE Trans. Antennas Propag.* **2015**, *63*, 1581–1588. [CrossRef]
36. Sabban, A. Wearable circular polarized antennas for health care, 5G, energy harvesting, and IoT systems. *Electronics* **2022**, *11*, 427. [CrossRef]
37. Mavaddat, A.; Armaki, S.H.M.; Erfanian, A.R. Millimeter-wave energy harvesting using 4×4 microstrip patch antenna array. *IEEE Antennas Wirel. Propag. Lett.* **2015**, *14*, 515–518. [CrossRef]
38. Gibson, P.J. The Vivaldi aerial. In Proceedings of the 9th European Conference, Brighton, UK, 17–20 September 1979; pp. 101–105.
39. Schneider, J.; Mrnka, M.; Gamec, J.; Gamcova, M.; Raida, Z. Vivaldi antenna for RF energy harvesting. *Radioengineering* **2016**, *25*, 666–671. [CrossRef]
40. Shi, Y.; Jing, J.; Fan, Y.; Yang, L.; Pang, J.; Wang, M. Efficient RF energy harvest with novel broadband Vivaldi rectenna. *Microw. Opt. Technol. Lett.* **2018**, *60*, 2420–2425.
41. Dong, Y.; Choi, J.; Itoh, T. Vivaldi antenna with pattern diversity for 0.7 to 2.7 GHz cellular band applications. *IEEE Antennas Wirel. Propag. Lett.* **2018**, *17*, 247–250. [CrossRef]
42. Agarwal, S.; Gupta, R.D.; Parihar, M.S.; Kondekar, P.N. A wideband and high gain dielectric resonator antenna for the RF energy harvesting application. *AEUE-Int. J. Electron. Commun.* **2017**, *78*, 24–31. [CrossRef]
43. Meher, P.R.; Behera, B.R.; Mishra, S.K. A compact circularly polarized cubic DRA with unit-step feed for Bluetooth/ISM/Wi-Fi/Wi-MAX applications. *AEUE-Int. J. Electron. Commun.* **2021**, *128*, 153521. [CrossRef]
44. Meher, P.R.; Behera, B.R.; Mishra, S.K.; Althuwayb, A.A. Design and analysis of a compact circularly polarized DRA for off-body communications. *AEUE-Int. J. Electron. Commun.* **2021**, *138*, 153880. [CrossRef]
45. Surender, D.; Halimi, M.A.; Khan, T.; Talukdar, F.A.; Antar, Y.M. Circularly polarized DR-rectenna for 5G and Wi-Fi bands RF energy harvesting in smart city applications. *IETE Tech. Rev.* **2021**, *39*, 890–893. [CrossRef]
46. Kraus, J.D. The helical antenna. *Proc. IRE* **1949**, *37*, 263–272. [CrossRef]
47. Rahim, R.A.; Hassan, S.I.S.; Malek, F.; Junita, M.N.; Jamlos, M.F. An investigation of ambient radio frequency as a candidate for energy harvesting source. In Proceedings of the IEEE Symposium on Industrial Electronics and Applications, Bandung, Indonesia, 25–28 September 2012; pp. 95–99.
48. Shi, Y.; Jing, J.; Fan, Y.; Yang, L.; Wang, M. Design of a novel compact and efficient rectenna for Wi-Fi energy harvesting. *Prog. Electromagn. Res. C* **2018**, *83*, 57–70. [CrossRef]
49. Alex-Amor, A.; Palomares-Caballero, Á.; Fernández-González, J.M.; Padilla, P.; Marcos, D.; Sierra-Castañer, M.; Esteban, J. RF energy harvesting system based on an archimedean spiral antenna for low-power sensor applications. *Sensors* **2019**, *19*, 1318. [CrossRef] [PubMed]
50. Sun, Y.; Zhang, H.; Wen, G.; Wang, P. Research progress in Yagi antenna. *Procedia Eng.* **2012**, *29*, 2116–2121. [CrossRef]
51. Sun, H.; Guo Y.X.; He, M.; Zhong, Z. A dual-band rectenna using broadband Yagi antenna array for ambient RF power harvesting. *IEEE Antennas Wirel. Propag. Lett.* **2013**, *12*, 918–921. [CrossRef]
52. Popović, Z.; Korhummel, S.; Dunbar, S.; Scheeler, R.; Dolgov, A.; Zane, R.; Falkenstein, E.; Hagerty, J. Scalable RF energy harvesting. *IEEE Trans. Microw. Theory Tech.* **2014**, *62*, 1046–1056. [CrossRef]
53. Elkhosht, R.; Hammad, H. A dualband rectenna design for RF energy scavenging using a modified yagi-uda antenna. In Proceedings of the International Microwave and Antenna Symposium (IMAS), Cairo, Egypt, 7–9 February 2023; pp. 154–157.
54. Hamadameen, J.A. Analysis, design and simulation of the log periodic antenna for mobile communication bands. *WSEAS Trans. Commun.* **2008**, *7*, 399–402.
55. Kumar, H.; Arrawatia, M.; Kumar, G. Broadband planar log-periodic dipole array antenna based RF-energy harvesting system. *IETE J. Res.* **2019**, *65*, 39–43. [CrossRef]
56. Khaliq, H.S.; Awais, M.; Ahmad, W.; Khan, W.T. A high gain six band frequency independent dual CP planar log periodic antenna for ambient RF energy harvesting. In Proceedings of the Progress In Electromagnetics Research Symposium-Fall, Singapore, 19–22 November 2017; pp. 3024–3028.
57. Roy, S.; Tiang, J.-J.; Roslee, M.B.; Ahmed, M.T.; Kouzani, A.Z.; Mahmud, M.A.P. Design of a highly efficient wideband multi-frequency ambient RF energy harvester. *Sensors* **2022**, *22*, 424. [CrossRef]
58. Erkmen, F.; Almoneef, T.S.; Ramahi, O.M. Scalable electromagnetic energy harvesting using frequency selective surfaces. *IEEE Trans. Microw. Theory Tech.* **2018**, *66*, 2433–2441. [CrossRef]
59. Palazzi, V.; Hester, J.; Bito, J.; Alimenti, F.; Kalialakis, C.; Collado, A.; Mezzanotte, P.; Georgiadis, A.; Roselli, L.; Tentzeris, M.M. A novel ultra-lightweight multiband rectenna on paper for RF energy harvesting in the next generation LTE Bands. *IEEE Trans. Microw. Theory Tech.* **2018**, *66*, 366–379. [CrossRef]
60. Awasis, Q.; Jin, Y.; Chattha, H.T.; Jamil, M.; Qiang, H.; Khawaja, B.A. A compact rectenna system with high conversion efficiency for wireless energy harvesting. *IEEE Access* **2018**, *6*, 35857–35866. [CrossRef]
61. Adami, S.E.; Proynov, P.; Hilton, G.S.; Yang, G.; Zhang, C.; Zhu, D.; Li, Y.; Beeby, S.P.; Craddock, I.J.; Stark, B.H. A flexible 2.45-GHz power harvesting wristband with net system output from -24.3 dBm of RF power. *IEEE Trans. Microw. Theory Tech.* **2018**, *66*, 380–395. [CrossRef]
62. Fowler, C.; Zhou, J. A metamaterials inspired approach to RF energy harvesting. *Appl. Phys.* **2017**, 1–11. [CrossRef]

63. Lee, W.; Choi, S.-I.; Kim, H.-I.; Hwang, S.; Jeon, S.; Yoon, Y.-K. Metamaterial-integrated high-gain rectenna for RF sensing and energy harvesting applications. *Sensors* **2021**, *21*, 6580. [CrossRef]
64. Sun, Z.; Zhao, X.; Zhang, L.; Mei, Z.; Zhong, H.; You, R.; Lu, W.; You, Z.; Zhao, J. WiFi energy-harvesting antenna inspired by the resonant magnetic dipole metamaterial. *Sensors* **2022**, *22*, 6523. [CrossRef]
65. Badawe, M.E.I.; Ramahi, O.M. Efficient metasurface rectenna for electromagnetic wireless power transfer and energy harvesting. *Prog. Electromagn. Res.* **2018**, *161*, 35–40. [CrossRef]
66. Nasimuddin, N.; Cheng, Z.N.; Qing, X. Bandwidth enhancement of a single-feed circularly polarized antenna using metasurface. *IEEE Antennas Propag. Mag.* **2016**, *58*, 39–46. [CrossRef]
67. Agarwal, K.; Nasimuddin, N.; Alphones, A. Wideband circularly polarized AMC reflector backed aperture antenna. *IEEE Trans. Antennas Propag.* **2016**, *61*, 1456–1461. [CrossRef]
68. Vignesh, S.B.; Nasimuddin, N.; Alphones, A. Stubs-integrated-microstrip antenna design for wide coverage of circularly polarised radiation. *IET Microw. Antennas Propag.* **2017**, *11*, 444–449. [CrossRef]
69. Nguyen, H.Q.; Le, M.T. Multiband ambient RF energy harvester with high gain wideband circularly polarized antenna toward self-powered wireless sensors. *Sensors* **2021**, *21*, 7411. [CrossRef]
70. Olgun, U.; Chen, C.C.; Volakis, J.L. Investigation of rectenna array configurations for enhanced RF power harvesting. *IEEE Antennas Wirel. Propag. Lett.* **2011**, *10*, 262–265. [CrossRef]
71. Alwareth, H.; Ibrahim, I.M.; Zakaria, Z.; Al-Gburi, A.J.A.; Ahmed, S.; Nasser, Z.A. A wideband high-gain microstrip array antenna integrated with frequency-selective surface for sub-6 GHz 5G applications. *Micromachines* **2022**, *13*, 1215. [CrossRef] [PubMed]
72. Li, Y.; Jandhyala, V. Design of retrodirective antenna arrays for short-range wireless power transmission. *IEEE Trans. Antennas Propag.* **2012**, *60*, 206–211. [CrossRef]
73. Yang, X.; Geyi, W.; Sun, H. Optimum design of wireless power transmission system using microstrip patch antenna arrays. *IEEE Antennas Wirel. Propag. Lett.* **2017**, *16*, 1824–1827. [CrossRef]
74. Li, Y.; Rajendran, J.; Mariappan, S.; Rawat, A.S.; Sal Hamid, S.; Kumar, N.; Othman, M.; Nathan, A. CMOS radio frequency energy harvester (RFEH) with fully on-chip tunable voltage-booster for wideband sensitivity enhancement. *Micromachines* **2023**, *14*, 392. [CrossRef]
75. Pakkirisami Churchill, K.K.; Ramiah, H.; Chong, G.; Chen, Y.; Mak, P.-I.; Martins, R.P. A fully-integrated ambient RF energy harvesting system with 423-µW output power. *Sensors* **2022**, *22*, 4415. [CrossRef]
76. Benkalfate, C.; Ouslimani, A.; Kasbari, A.-E.; Feham, M. A new RF energy harvesting system based on two architectures to enhance the DC output voltage for WSN feeding. *Sensors* **2022**, *22*, 3576. [CrossRef]
77. Halimi, M.A.; Shome, P.P.; Khan, T.; Rengarajan, S.R. Efficient single and broadband microwave rectifiers for RFEH/WPT enabled low power 5G sub-6 GHz devices. *AEUE-Int. J. Electron. Commun.* **2023**, *165*, 154645. [CrossRef]
78. Ge, L.; Luk, K. Frequency-reconfigurable low-profile circular monopolar patch antenna. *IEEE Trans. Antennas Propag.* **2014**, *62*, 3443–3449.
79. Magray, M.I.; Muzaffar, K.; Wani, Z.; Singh, R.K.; Karthikeya, G.S.; Koul, S.K. Compact frequency reconfigurable triple band notched monopole antenna for ultrawideband applications. *Int. J. RF Microw. Comput.-Aided Eng.* **2019**, *29*, e29142. [CrossRef]
80. Muthuvel, S.K.; Choukiker, Y.K. Frequency tunable circularly polarized antenna with branch line coupler feed network for wireless applications. *Int. J. RF Microw. Comput.-Aided Eng.* **2019**, *29*, e21784. [CrossRef]
81. Idris, I.H.; Hamid, M.R.; Kamardin, K.; Rahim, M.K.A. A multi to wideband frequency reconfigurable antenna. *Int. J. RF Microw. Comput.-Aided Eng.* **2018**, *28*, e21216. [CrossRef]
82. Yang, X.; Shao, B.-C.; Yang, F.; Elsherbeni, A.Z.; Gong, B. A polarization reconfigurable patch antenna with loop slots on the ground plane. *IEEE Antennas Wirel. Propag. Lett.* **2012**, *11*, 69–72. [CrossRef]
83. Chen, C.; Sim, C.; Lin, H. Annular ring slot antenna design with reconfigurable polarization. *Int. J. RF Microw. Comput.-Aided Eng.* **2016**, *26*, 110–120. [CrossRef]
84. Bagheroghli, H.; Zaker, R. Double triangular monopole-like antenna with reconfigurable single/dual-wideband circular polarization. *Int. J. RF Microw. Comput.-Aided Eng.* **2018**, *28*, e21267. [CrossRef]
85. Tran, H.H.; Park, H.C. Wideband polarization reconfigurable circularly polarized antenna with omnidirectional radiation pattern. *Int. J. RF Microw. Comput.-Aided Eng.* **2019**, *29*, e21708. [CrossRef]
86. Zhang, G.; Hong, J.-S.; Song, G.; Wang, B.-Z. Design and analysis of a compact wideband pattern-reconfigurable antenna with alternate reflector and radiator. *IET Microw. Antennas Propag.* **2012**, *6*, 1629–1635. [CrossRef]
87. Row, J.; Wu, Y. Pattern reconfigurable slotted-patch array. *IEEE Trans. Antennas Propag.* **2018**, *66*, 1580–1583. [CrossRef]
88. Saurav, K.; Sarkar, D.; Srivastava, K.V. Multi-band pattern reconfigurable Yagi-Uda antenna. *Int. J. RF Microw. Comput.-Aided Eng.* **2017**, *27*, e21116. [CrossRef]
89. Ghaffar, A.; Li, X.J.; Awan, W.A.; Naqvi, A.H.; Hussain, N.; Alibakhshikenari, M.; Limiti, E. A flexible and pattern reconfigurable antenna with small dimensions and simple layout for wireless communication systems operating over 1.65–2.51 GHz. *Electronics* **2021**, *10*, 601. [CrossRef]
90. Zainarry, S.N.M.; Nguyen-Trong, N.; Fumeaux, C. A high-gain dual-band directional/omnidirectional reconfigurable antenna for WLAN systems. *IEEE Antennas Wirel. Propag. Lett.* **2018**, *17*, 617–620. [CrossRef]

91. Iqbal, A.; Smida, A.; Mallat, N.K.; Ghayoula, R.; Elfergani, I.; Rodriguez, J.; Kim, S. Frequency and pattern reconfigurable antenna for emerging wireless communication systems. *Electronics* **2019**, *8*, 407. [CrossRef]
92. Koutinos, A.; Xanthopoulou, G.; Kyriacou, G.; Chryssomallis, M. A reconfigurable polarization-frequency supershape patch antenna with enhanced bandwidth. *Electronics* **2020**, *9*, 1166. [CrossRef]
93. Sharma, A.; Rathi, A.; Al-Khafaji, H.M.R.; Siddiqui, M.G.; Yadav, A.K.S. Hybrid mode reconfigurable antenna with V-shaped extrudes for cognitive radio applications. *Electronics* **2023**, *12*, 1680. [CrossRef]
94. Hussain, R.; Khan, M.U.; Sharawi, M.S. An integrated dual MIMO antenna system With dual-function GND-plane frequency-agile antenna. *IEEE Antennas Wirel. Propag. Lett.* **2018**, *17*, 142–145. [CrossRef]
95. Pan, Y.; Ma, Y.; Xiong, J.; Hou, Z.; Zeng, Y. A compact antenna with frequency and pattern reconfigurable characteristics. *Microw. Opt. Technol. Lett.* **2015**, *57*, 2467–2471. [CrossRef]
96. Quin, P.-Y.; Guo, Y.J.; Weily, A.R.; Liang, C.-H. A pattern reconfigurable U-Slot antenna and its applications in MIMO systems. *IEEE Trans. Antennas Propag.* **2012**, *60*, 516–528. [CrossRef]
97. Han, L.; Cheng, G.; Han, G.; Zhang, W. Reconfigurable ultra-wideband monopole antenna with single-, dual-, and triple-band notched functions. *Int. J. RF Microw. Comput.-Aided Eng.* **2019**, *29*, e21837. [CrossRef]
98. Tawk, Y.; Costantine, J.; Hemmady, S.; Balakrishnan, G.; Avery, K.; Christodoulou, C.G. Demonstration of a cognitive radio front end using an optically pumped reconfigurable antenna system (OPRAS). *IEEE Trans. Antennas Propag.* **2012**, *60*, 1075–1083. [CrossRef]
99. Tawk, Y.; Albrecht, A.R.; Hemmady, S.; Balakrishnan, G.; Christodoulou, C.G. Optically pumped frequency reconfigurable antenna design. *IEEE Antennas Wirel. Propag. Lett.* **2010**, *9*, 280–283. [CrossRef]
100. Sathi, V.; Ehtheshami, N.; Nourinia, J. Optically tuned frequency reconfigurable microstrip antenna. *IEEE Antennas Wirel. Propag. Lett.* **2012**, *11*, 1018–1020. [CrossRef]
101. Jin, G.; Zhang, D.; Li, R. Optically controlled reconfigurable antenna for cognitive radio applications. *Electron. Lett.* **2011**, *47*, 948–950. [CrossRef]
102. Kamran Saleem, M.; Alkanhal, M.A.; Sheta, A.F. Switched beam dielectric resonator antenna array with six reconfigurable radiation patterns. *Int. J. RF Microw. Comput.-Aided Eng.* **2016**, *26*, 519–530. [CrossRef]
103. Rodrigo, D.; Jofre, L.; Cetiner, B. Circular beam-steering reconfigurable antenna with liquid metal parasitics. *IEEE Trans. Antennas Propag.* **2012**, *60*, 1796–1802. [CrossRef]
104. Mehdipour, A.; Denidni, T.A.; Sebak, A.-R.; Trueman, C.W.; Rosca, L.D.; Hoa, S.V. Mechanically reconfigurable antennas using anisotropic carbon-fibre composite ground. *IET Microw. Antennas Propag.* **2013**, *7*, 1055–1063. [CrossRef]
105. Liyakath, R.A.; Takshi, A.; Mumcu, G. Multilayer stretchable conductors on polymer substrates for conformal and reconfigurable antennas. *IEEE Antennas Wirel. Propag. Lett.* **2013**, *13*, 603–606. [CrossRef]
106. Azizi, M.K.; Ksiksi, M.A.; Ajlani, H.; Gharsallah, A. Terahertz graphene-based reconfigurable patch antenna. *Prog. Electromagn. Res. Lett.* **2017**, *71*, 69–76. [CrossRef]
107. Hlali, A.; Houaneb, Z.; Zair, H. Dual-band reconfigurable graphene-based patch antenna in terahertz band: Design, analysis and modeling using WCIP method. *Prog. Electromagn. Res. C* **2018**, *87*, 213–226. [CrossRef]
108. Liu, L.; Langley, R.J. Liquid crystal tunable microstrip patch antenna. *Electron. Lett.* **2008**, *44*, 1179–1180. [CrossRef]
109. Liu, G.B.; Zeng, L.; Huang, T.; Zhang, H. A tunable wide-band omnidirectional circularly polarized antenna regulated by the gravity field. *Int. J. RF Microw. Comput.-Aided Eng.* **2019**, *29* e21891. [CrossRef]
110. Lu, P.; Yang, X.-S.; Li, J.-L.; Wang, B.Z. Polarization reconfigurable broadband rectenna with tunable matching network for microwave power transmission. *IEEE Trans. Antennas Propag.* **2016**, *64*, 1136–1141. [CrossRef]
111. Lu, P., Yang, X.-S.; Li, J.-L.; Wang, B.Z. A compact frequency reconfigurable rectenna for 5.2- and 5.8-GHz wireless power transmission. *IEEE Trans. Power Electron.* **2015**, *30*, 6006–6010. [CrossRef]
112. Lu, P., Huang, K.M.; Yang, Y.; Cheng, F.; Wu, L. Frequency-reconfigurable rectenna with an adaptive matching stub for microwave power transmission. *IEEE Antennas Wirel. Propag. Lett.* **2019**, *18*, 956–960. [CrossRef]
113. Chuma, E.L.; Iano, Y.; Costa, M.S.; Manera, L.T.; Roger, L.L.B. A compact-integrated reconfigurable rectenna array for RF power harvesting with a practical physical structure. *Prog. Electromagn. Res. M* **2018**, *70*, 89–98.
114. Arun, V.; Karl Max, L.R. Micro-controlled tree shaped reconfigurable patch antenna with RF-energy harvesting. *Wirel. Pers. Commun.* **2017**, *94*, 2769–2781. [CrossRef]
115. Lu, P.; Yang, X.; Wang, B. A two-channel frequency reconfigurable rectenna for microwave power transmission and data communication. *IEEE Trans. Antennas Propag.* **2017**, *65*, 6976–6985. [CrossRef]
116. Lu, P.; Yang, X.-S.; Wang, B.-Z. Reconfigurable rectenna array design with mutual coupling analysis. *Microw. Opt. Technol. Lett.* **2019**, *61*, 654–659. [CrossRef]
117. Haung, F.; Yo, T.-C.; Lee, C.-M.; Luo, C.-H. Design of circular polarization antenna with harmonic suppression for rectenna application. *IEEE Antennas Wirel. Propag. Lett.* **2012**, *11*, 592–595.
118. Quddious, A.; Abbasi, M.A.B.; Saghir, A.; Arain, S.; Antoniades, M.A.; Polycarpou, A.; Vryonides, P.; Nikolaou, S. Dynamically reconfigurable SIR filter using rectenna and active booster. *IEEE Trans. Microw. Theory Tech.* **2019**, *67*, 1504–1515. [CrossRef]
119. Quddious, A.; Abbasi, M.A.B.; Tahir, F.A.; Antoniades, M.A.; Vryonides, P.; Nikolaou, S. UWB antenna with dynamically reconfigurable notch band using rectenna and active booster. *IET Microw. Antennas Propag.* **2019**, *13*, 2046–2052. [CrossRef]

120. Chou, J.; Lin, D.-B.; Weng, K.-L.; Li, H.-J. All polarization receiving rectenna with harmonic rejection property for wireless power transmission. *IEEE Trans. Antennas Propag.* **2014**, *62*, 5242–5249. [CrossRef]
121. Sun, H.; Geyi, W. A new rectenna with all-polarization-receiving capability for wireless power transmission. *IEEE Antennas Wirel. Propag. Lett.* **2016**, *15*, 814–817. [CrossRef]
122. Lin, W.; Ziolkowski, R.W.; Huang, J. Electrically small, low-profile, highly efficient, huygens dipole rectennas for wirelessly powering internet-of-things devices. *IEEE Trans. Antennas Propag.* **2019**, *67*, 3670–3679. [CrossRef]
123. Ren, Y.J.; Chang, K. 5.8-GHz circularly polarized dual-diode rectenna and rectenna array for microwave power transmission. *IEEE Trans. Microw. Theory Tech.* **2006**, *54*, 1495–1502.
124. Bertacchini, A.; Larcher, L.; Maini, M.; Vincetti, L.; Scorcioni, S. Reconfigurable RF energy harvester with customized differential PCB antenna. *J. Low Power Electron. Appl.* **2015**, *5*, 257–273. [CrossRef]
125. Lu, P.; Yang, X. Pattern reconfigurable rectenna with omni-directional/directional radiation modes for MPT with multiple transmitting antennas. *IEEE Microw. Wirel. Components Lett.* **2019**, *29*, 826–829. [CrossRef]
126. Kang, Z.; Lin, X.; Tang, C.; Mei, P.; Liu, W.; Fan, Y. 2.45-GHz wideband harmonic rejection rectenna for wireless power transfer. *Int. J. Microw. Wirel. Technol.* **2019**, *9*, 977–983. [CrossRef]
127. Hong, W.; Cao, Y.; Deng, L.; Li, S.; Li, M.; Liu, H. A circular polarized rectenna with out-of-band suppression for microwave power transmission. *Int. J. Antennas Propag.* **2016**, *2016*, 8628496. [CrossRef]
128. Kumar, D.; Chaudhary, K. Design of differential source fed circularly polarized rectenna with embedded slots for harmonics suppression. *Prog. Electromagn. Res. C* **2018**, *84*, 175–187. [CrossRef]
129. Ren, Y.; Farooqui, M.F.; Chang, K. A compact dual-frequency rectifying antenna with high-order harmonic-rejection. *IEEE Trans. Antennas Propag.* **2007**, *55*, 2110–2113. [CrossRef]
130. Elsheakh, D.N.; Elsadek, H.A.; Abdallah, E.A. Reconfigurable microstrip monopole patch antenna with electromagnetic band-gap structure design for ultrawideband wireless communication systems. *Microw. Opt. Technol. Lett.* **2011**, *53*, 2466–2471. [CrossRef]
131. Lee, D.; Lee, S.-J.; Hwang, I.-J.; Lee, W.-S.; Yu, J.-W. Hybrid power combining rectenna array for wide incident angle coverage in RF energy transfer. *IEEE Trans. Microw. Theory Tech.* **2017**, *65*, 3409–3418. [CrossRef]
132. Ashtari, R.; Baginski, M.; Dean, R. A 2.45-GHz frequency-selective rectenna for wireless energy harvesting. *Microw. Opt. Technol. Lett.* **2019**, *58*, 2508–2512. [CrossRef]
133. Harouni, Z.; Osman, L.; Gharsallah, A. Efficient 2.45 GHz rectenna design with high harmonic rejection for wireless power transmission. *Int. J. Comput. Sci.* **2010**, *7*, 424–427.
134. Shah, I.A.; Hayat, S.; Basir, A.; Zada, M.; Shah, S.A.A.; Ullah, S. Design and analysis of a hexa-band frequency reconfigurable antenna for wireless communication. *AEUE-Int. J. Electron. Commun.* **2019**, *98*, 80–88. [CrossRef]
135. Ali, M.; Yang, G.; Dougal, R. A new circularly polarized rectenna for wireless power transmission and data communication. *IEEE Antennas Wirel. Propag. Lett.* **2005**, *4*, 205–208. [CrossRef]
136. Pal, H.; Choukiker, Y.K. Design of frequency reconfigurable antenna with ambient RF-energy harvester system. In Proceedings of the 2016 IEEE International Conference on Information Communication and Embedded Systems, Chennai, India, 25–26 February 2016; pp. 1–5.
137. Anuradha, A.P.; Lahudkar, S.L. Compact asymmetric fractal frequency and pattern reconfigurable monopole antenna. *AEUE-Int. J. Electron. Commun.* **2019**, *111*, 152915.
138. Tsai, J.; Row, J. Design of frequency sensor based on reconfigurable rectenna. *Microw. Opt. Technol. Lett.* **2014**, *56*, 1739–1742. [CrossRef]
139. Harouni, Z.; Cirio, L.; Osman, L.; Gharsallah, A.; Picon, O. A dual circularly polarized 2.45-GHz rectenna for wireless power transmission. *IEEE Antennas Wirel. Propag. Lett.* **2011**, *10*, 306–309. [CrossRef]
140. Li, K.; Cai, Y.-M.; Yin, Y.; Hu, W. A wideband E-plane pattern reconfigurable antenna with enhanced gain. *Int. J. RF Microw. Comput.-Aided Eng.* **2019**, *29*, e21530. [CrossRef]
141. Ledimo, B.K.; Moaro, P.; Ramogomana, R.; Mosalaosi, M.; Basutli, B. Design procedure of a frequency reconfigurable metasurface antenna at mmwave band. *Telecom* **2022**, *3*, 379–395. [CrossRef]
142. Jiang, S.; Liu, Z.; Yang, H.; Sun, D. A single-layer multimode metasurface antenna with a CPW-fed aperture for UWB communication applications. *Micromachines* **2023**, *14*, 249. [CrossRef]
143. Le, T.T.; Tran, H.H.; Althuwayb, A.A. Wideband circularly polarized antenna based on a non-uniform metasurface. *Appl. Sci.* **2020**, *10*, 8652. [CrossRef]
144. Hao, H.; Wang, S.; Gao, H.; Ma, X.; Huang, X. Low-cost broadband circularly polarized array antenna with artificial magnetic conductor for indoor applications. *Appl. Sci.* **2023**, *13*, 3104. [CrossRef]
145. Meher, P.R.; Behera, B.R.; Mishra, S.K.; Althuwayb, A.A. A chronological review of circularly polarized dielectric resonator antenna: Design and developments. *Int. J. RF Microw. Comput.-Aided Eng.* **2021**, *31*, e22589. [CrossRef]
146. Meher, P.R.; Behera, B.R.; Mishra, S.K. Broadband circularly polarized edge feed rectangular dielectric resonator antenna using effective glueless technique. *Microw. Opt. Technol. Lett.* **2020**, *62*, 3333–3341. [CrossRef]
147. Mohanty, A.; Behera, B.R. Dynamically switched dual-band dual-polarized dual-sense low-profile compact slot circularly polarized antenna assisted with high gain reflector for sub-6GHz and X-band applications. *Prog. Electromagn. Res. C* **2021**, *110*, 197–212. [CrossRef]

148. Behera, B.R.; Mohanty, A.; Nasimuddin, N. Dual-polarized metasurface-based monopole antenna design using characteristics mode theory for UHF RFID applications. *Int. J. RF Microw. Comput.-Aided Eng.* **2022**, *32*, e23325. [CrossRef]
149. Luo, Y.; Pu, L.; Wang, G.; Zhao, Y. RF energy harvesting wireless communications: RF environment, device hardware and practical issues. *Sensors* **2019**, *19*, 3010. [CrossRef] [PubMed]
150. Mouapi, A. Radiofrequency energy harvesting systems for internet of things applications: A comprehensive overview of design issues. *Sensors* **2022**, *22*, 8088. [CrossRef]
151. Alsharif, M.H.; Kim, S.; Kuruoğlu, N. Energy harvesting techniques for wireless sensor networks/radio-frequency identification: A review. *Symmetry* **2019**, *11*, 865. [CrossRef]
152. Ahmad, I.; Dildar, H.; Khan, W.U.R.; Shah, S.A.A.; Ullah, S.; Ullah, S.; Umar, S.M.; Albreem, M.A.; Alsharif, M.H.; Vasudevan, K. Design and experimental analysis of multiband compound reconfigurable 5G antenna for sub-6 GHz wireless applications. *Wirel. Commun. Mob. Comput.* **2021**, *2021*, 5588105 [CrossRef]
153. Ahmad, I.; Dildar, H.; Khan, W.U.R.; Ullah, S.; Ullah, S.; Albreem, M.A.; Alsharif, M.H.; Uthansakul, P. Frequency reconfigurable antenna for multi standard wireless and mobile communication systems. *Comput. Mater. Contin.* **2021**, *68*, 2563–2578. [CrossRef]
154. Alsharif, M.H.; Hossain, M.; Jahid, A.; Khan, M.A.; Choi, B.J.; Mostafa, S.M. Milestones of wireless communication networks and technology prospect of next generation (6g). *Comput. Mater. Contin.* **2022**, *71*, 4803–4818. [CrossRef]
155. Alsharif, M.H.; Jahid, A.; Kelechi, A.H.; Kannadasan, R. Green IoT: A review and future research directions. *Symmetry* **2023**, *15*, 757. [CrossRef]